An Analytical Study of Slug Impact Phenomena

B.L. Smith
Swiss Federal Institute for Reactor Research, CH-5303 Würenlingen, Switzerland

Following an HCDA the roof of a fast reactor may be threatened by coolant impact. Large computer codes are used to analyse model experiments in which roof impact situations occur, but discrepancies between prediction and measurement have given rise to some misgivings over the usefulness of the numerical models. In most instances experimental roof assemblies are made over-strong in order to simulate a fixed roof configuration to simplify the analysis. Recent trends in pool-type LMFBR roof designs however, do not preclude the possibility of structural response during the impact process. Such roof motions could have a feed-back effect on the hydrodynamic loading due to fluid-structure interactions.

This article aims to develop at a fundamental level, understanding of the impact process and assess the relevance and magnitude of fluid-structure interaction effects. Reference is made for four 1/30th scale experiments, set up to verify the ideas developed in this work, and to provide quality data for code validation purposes.

The impact of a one-dimensional liquid slug on a solid slab is investigated using a simplified form of the Rankine-Hugoniot shock equations derived under the joint assumptions of slight compressibility and small Mach number; both assumptions are well justified for the applications in mind.

In the first instance the roof slab is considered to be freely supported and of finite thickness. A detailed picture of the shock and expansion wave propagations is built up from the basic equations including the effects of wave reflections at boundaries and wave-wave interactions. Particular attention is paid to the impulse transfer mechanism from the slug as this controls the roof slab acceleration. Bulk fluid cavitation effects are noted.

Roof flexural response is then taken into account, together with the effects the hold-down constraints. It is seen that even very minor structural responses can result in significant mitigation of the impulse loading.

Guidelines for the application of the work to HCDA analysis in pool reactor geometries is presented.

1. Introduction

A number of large computer codes have been developed which aim to assess the strength of a fast reactor primary containment against internal pressurization resulting from an HCDA. It is now recognized that uncoupled analyses of core energetics, coolant and structural responses can result in overly pessimistic and often misleading conclusions. As a consequence, most codes have the capacity to simultaneously compute the structural loading and the structural responses in order to take into account any mutual interactions which might occur.

One of the significant loading events associated with an HCDA concerns the impact of an accelerated sodium slug on the underside of the reactor roof. The purpose of the present paper is to develop an understanding of the impact process and to assess the character and importance of the fluid/structure interaction effects.

We start by considering the (one-dimensional) impact of a liquid slug on a freely-supported roof slab of finite thickness and compressibility. The effects of roof hold-down are then included, at first as a rigid constraint, but then as an elastic support. As an application of the work, reference is made to a recent series of flexible roof experiments carried out at AEE Winfrith*.

2. Basic Equations

The fluid regime in which our analysis is based enables several simplifications to be made. Liquids such as water and sodium are only slightly compressible and for our applications the Mach number is also small. In these circumstances the standard conservation equations of mass and momentum may be linearized to give, in one dimension,

$$\frac{\partial P}{\partial t} + \rho_0 c^2 \frac{\partial v}{\partial z} = 0 \quad : \quad \rho_0 \frac{\partial v}{\partial t} + \frac{\partial P}{\partial z} = 0 \tag{1}$$

where P, v denote pressure and velocity, ρ_0 is the undisturbed density and $c^2 = \frac{\partial P}{\partial \rho}$. The equations integrate immediately:

$$P = \rho_0 c \left[F(z-ct) - G(z+ct)\right]; \quad v = F(z-ct) + G(z+ct) \tag{2}$$

in which F and G are arbitrary functions representing wave propogations in the positive and negative z directions respectively.

In slug impact situations it will be necessary to take account of discontinuities in the flow field. The Rankine-Hugoniot jump conditions apply in these circumstances, and in our case these may also be simplified to give

$$P_1 - \rho_0 c v_1 = P_2 - \rho_0 c v_2 \tag{3}$$

where the subscripts refer to the regions either side of the discontinuity. All velocities are considered positive in the direction of increasing z.

Applications of the basic continuum equations (2), (3) to various slug impact situations are considered in the following sections. We begin with the conservative case of impact of a liquid slug on a rigid, fixed roof; an approach commonly used in reactor safety analyses for obtaining roof impulse loads.

3. Fixed Roof Model

Consider the situation illustrated in Figure 1(a) in which a liquid slug of length L, driven upwards at velocity U by an expanding core bubble, impacts on the reactor roof, here

---

* The author is indebted to Dr. M.J. Lancefield for making available experimental information prior to publication.

regarded as fixed and rigid.

Upon impact a shock wave develops at the surface of contact and propogates down the liquid column, as depicted in Fig. 1(b). The physical state of the shocked liquid denoted as region 1 in the Figure, may be calculated from the basic equations (2) and (3) together with the boundary condition

$$v = 0 \quad \text{at} \quad z = 0 , \tag{4}$$

applied at the liquid/roof interface. This gives

$$P_1 = \rho_0 cU \quad ; \quad v_1 = 0 \tag{5}$$

In other words, as a result of the impact the liquid column is brought to rest and the impact pressure is $\rho_0 cU$; a well-known result.

The shock is reflected as an expansion wave at the free surface at the base of the liquid column, Fig. 1(c). This wave travels up the column as indicated, and the pressure and velocity behind it are simply:

$$P_2 = 0, \quad v_2 = -U \tag{6}$$

these being the appropriate solutions of the basic equation assuming negligible pressure at the liquid/bubble boundary.

In Fig. 1(d) the reflected expansion wave has reached the upper surface of the column and "plucked" the liquid from the roof producing local cavitation at the contact surface. At the end of the impact the liquid column moves downwards at uniform velocity U and it is easily shown that the impulse delivered to the roof is

$$I = 2MU \tag{7}$$

where $M=\rho_0 L$ is the mass of the liquid. Fig. 1(e) shows the pressure transient for the interaction: a square pulse of amplitude $\rho_0 cU$.

4. Freely-Supported Roof Model

Replacing the fixed roof of the previous section by a freely-supported slab of finite compressibility produces very different behaviour. Fig. 2(a) shows an initial impact configuration in which the liquid column impinges upon an unrestrained roof slab of thickness $\tilde{L}$ and density $\tilde{\rho}$.

A shock wave propogates down the liquid column as in the previous example, but a similar wave is transmitted upwards into the roof slab, Fig. 2(b). The pressures behind the shock fronts are given by Relations (2) and depend on the acoustic impedance mismatch $\rho_0 c:\tilde{\rho}_0\tilde{c}$ between the two materials, this ratio being slightly smaller for water/steel interactions (1:24) than for sodium/steel interactions (1:20). Provided the roof slab is allowed to move freely, it transpires that the fluid/structure interaction is characterized completely in terms of the two fundamental parameters α, N defined by

$$\alpha = \frac{\rho_0 c}{\tilde{\rho}_0 \tilde{c}} \qquad N = \frac{L/c}{\tilde{L}/\tilde{c}} \tag{8}$$

The quantity α is the ratio of the acoustic impedances and N the ratio of the acoustic transit times, with the tildes indicating values for the roof slab and the zero subscript referring to the initial, undisturbed state.

The situation may be analysed using the basic equations (2), (3) together with the continuity conditions

$$P = \tilde{P} \; ; \; v = \tilde{v} \tag{9}$$

applicable at the contact surface. This gives for the regions (subscript 1) behind the shock fronts in Fig. 2(b):

$$P_1 = \tilde{P}_1 = \frac{1}{1+\alpha}\rho_0 cU \quad ; \quad v_1 = \tilde{v}_1 = \frac{\alpha}{1+\alpha} U \ . \tag{10}$$

Letting $\rho \rightarrow \infty$ $(\alpha \rightarrow 0)$ we recover the fixed roof values given in the last section. Allowing for finite roof material properties reduces the impact pressure by 4 % for a water/steel interaction and by 5 % for a sodium/steel interaction.

The transmitted wave in the roof is reflected as a rarefaction at the roof upper surface and travels back down towards the contact surface, Fig. 2(c). Conditions behind the wave front, Region 2 in the Figure, are given by

$$\tilde{P}_2 = 0 \quad ; \quad \tilde{v}_2 = \left[1-\left\{\frac{1-\alpha}{1+\alpha}\right\}\right] U. \tag{11}$$

At the contact surface the rarefaction reflects as a compression, but a rarefaction is transmitted into the liquid; see Fig. 2(d). We may derive the flow conditions behind the fronts as before:

$$P_3 = \tilde{P}_3 = \frac{(1-\alpha)}{(1+\alpha)^2}\rho_0 cU \quad ; \quad v_3 = \tilde{v}_3 \left[1 - \frac{(1-\alpha)}{(1+\alpha)^2}\right] U \tag{12}$$

Since the factor $(1-\alpha)/(1+\alpha) < 1$, Equations (12) indicate a reduction in pressure and an associated increase in velocity as a result of the wave reflections; c.f. Equations (10).

The reflected wave transits the roof as before to be further reflected as a rarefaction at the roof upper surface. At each reflection the interface pressure reduces by a factor $(1-\alpha)/(1+\alpha)$ while the roof motion is incremented by a corresponding amount. After a number of such transits the liquid column appears as in Fig. 2(e) with a train of waves moving downwards towards the free surface at the base of the column. The leading wave is compressive, being that resulting from the initial impact, while those following are expansion waves caused by multiple wave interactions at the slug/roof interface.

The leading compressive wave is turned round at the lower (free) surface and ascends the column as a rarefaction. Its interaction with the descending train of rarefactions produces tensions in the fluid and probably cavitation, depicted in Fig. 2(f); this appearing first near the base but ascending with the wavefront. Ultimately the ascending wave reaches the contact surface and separates the liquid from the roof, bringing the impact to an end and leaving the entire liquid column in a cavitated state, shown in Fig. 2(g). Note the contrast with the fixed roof case in which cavitation is localized at the slug/roof interface, Fig. 1(d). During the impact process the interface pressure decreases steadily as a result of multiple wave reflections (accompanied by increases in the interface velocity). This behaviour is seen in Fig. 2(h).

It is convenient, without being restrictive, to assume that the N in Equation (8) is an integer. In that case the impulse delivered to the roof slab during the impact phase is easily derived from a generalization of Equation (12) followed by an integration with respect to time. This gives

$$I = \frac{1}{N\alpha}\left[1-\left(\frac{1-\alpha}{1+\alpha}\right)^N\right] MU \tag{13}$$

and reduces to I=2MU for the fixed roof case, as expected.

A thin roof plate can be considered of negligible thickness but of finite mass. Effectively, wave propogation though the plate is instantaneous and the interface pressure decays smoothly rather than as the series of steps seen in Fig. 2(g). Equation (13) in this case reduces to

$$I = \frac{1}{N\alpha}\left[1 - \exp(-2\alpha N)\right] MU. \tag{14}$$

It transpires that the thin plate approximation is excellent for all the applications to reactor and scale model situations considered by the author; c.f. Table I.

We apply the formulae above to four roof models, chosen in order to vary independently the two fundamental parameters α, N of Equation (8). Two models are of steel, two of aluminium alloy, and the thicknesses are 15 cm and 3 cm for each material. A 15 cm thick steel roof is normally used as cover plate in the COVA series of experiments, [1], [2], some of which produce a one-dimensional fluid impact. We accordingly adopt a slug length L=40 cm, appropriate for experiments of this type. Table I compares impulse reductions (in units of MU) for each of the roof models against that for a fixed roof. The impulses entered in the fourth column are calculated from Equation (13), those in the fifth column from Equation (14). It will be seen that the thin-plate approximation is perfectly adequate for all these models.

It is worth remarking that an impulse transfer of MU or greater is required to arrest the upward motion of the liquid slug. The Table shows that this is achieved for both the steel and aluminium thick roof models so that in these cases the hydrodynamic loading is complete after a single impact. For the thin roof cases however, this is not true and the cavitated liquid column shown in Fig. 2(g) evidently retains a net upward velocity. Clearly, if the roof decelerates under the influence of its restraint devices, the liquid column will re-compress and reimpact to effect a further pressure loading and momentum transfer. This process will continue until sufficient momentum ($\gtrsim$ MU) has been transferred. Multiple impact phenomena for the thin roof models have been confirmed experimentally.

5. Fixed Support Roof Model

We considered in the last Section the impact of a liquid slug on an unsupported roof slab, that is, one in which roof hold-down effects may be ignored. In reactor situations as well as in model containment experiments, the roof cover is restrained in some manner near its outer rim. The stiffness of the roof will govern its flexural behaviour against the restraints, while the strength of the roof supports will determine the bulk motion. We will need to assess the relevance of both of these effects to the hydrodynamic loading.

We begin with the flexural behaviour and consider a circular roof plate, held fixed at the outer rim, subjected to impact loading from a rising liquid slug, Fig. 3(a). In realistic applications it is unlikely that the roof will strain by more than a few percent and this should not invalidate the assumed one-dimensionality of the slug motion. As we established in the previous Section, it is not necessary to follow explicitly the wave propogations through the roof and the thin-plate approximation is therefore adopted.

Upon impact a shock wave propogates down the liquid column and the roof plate flexes under the hydrodynamic load, Fig. 3(b). As is now familiar, the shock reflects as a rare-faction at the lower end of the column and this travels upwards to ultimately separate the liquid from the roof upon arrival at the contact surface, Fig. 3(c).

It is convenient to analyse the impact process by means of an equivalent spring system, the principles of which are illustrated in Figs. 3(d)-3(f). Following Szilard [3], we formulate an equivalence algorithm by which the load, mass and spring factors for the equivalent system may be related to those of the actual system, the transformation factors being derived by equating the kinetic and strain energies of the real and substitute systems, together with the works of the external forces. According to the linear theory for the vibration of a clamped circular plate, we find:

$$F_e = \frac{\pi a^2}{3} P \quad ; \quad M_e = \frac{\pi a^2}{5} \tilde{\rho} h \quad ; \quad K_e = \frac{64\pi}{3} \frac{D}{a^2} \tag{15}$$

where P is pressure, $\tilde{\rho}$ the plate density, a and h are the radius and thickness of the plate and D its flexural rigidity. The quantities F_e, M_e and K_e define respectively the total load, mass and spring constant to be used in the equation of motion for the equivalent system:

$$F_e - K_e \xi = M_e \ddot{\xi} \tag{16}$$

in which ξ is the displacement. The fundamental frequency of the equivalent system, $\omega_e = \sqrt{K_e/M_e}$ agrees closer than 1 % with the exact value given in Timoschenkö [4] for a clamped plate in free vibration.

The equivalent roof model may now be used to perform the fluid/structure analysis. Appropriate solutions of the basic equations (2), (3) for the region behind the shock front of Fig. 3(e) are

$$P_1 = \rho_0 c \left\{\frac{U}{2} - G(z+ct)\right\} \quad , \quad v_1 = \frac{U}{2} + G(z+ct) \tag{17}$$

The arbitrary function G may be eliminated between the Equations (17) to give, in particular, a relation between pressure and velocity at the contact surface, $z=\xi$:

$$P = \rho_0 c \; (U - \dot{\xi}) \tag{18}$$

This equation, in conjuction with (15), (16) becomes the equation of motion of the plate, and may be written in the form:

$$\ddot{\xi} + 2\lambda\dot{\xi} + \omega^2\xi = 2\lambda U, \quad \text{where } \lambda = \frac{5}{6} \frac{\rho_0 c}{\tilde{\rho} h} \quad , \quad \omega^2 = \frac{320}{3\tilde{\rho}} \frac{D}{ha^4} \tag{19}$$

in which it is easily recognized as the equation of a damped, linear oscillator. For a system disturbed from rest the solution for the pressure field is

$$P = \rho_0 cU \left\{1 - \frac{2}{k} \sin k\lambda t \; e^{-\lambda t}\right\} \quad , \quad \text{with} \quad k = \sqrt{\omega^2/\lambda^2 - 1} \tag{20}$$

A typical pressure transient for a thick plate (h=15 cm), derived from Equation (20) is given in Fig. 4(a) alongside that for an identical, but unsupported, plate, Fig. 4(b); dimensions are chosen appropriate to COVA geometry. As the motion is damped, and the pressure decreases initially, a small reduction in impulse compared to the rigid roof case will accompany the vibration. However, for the thick roof models the flexural rigidity is high enough that the impulse reduction is negligible (1/2 % for steel, 3 % for aluminium).

The pressure transient for a thin (h=3 cm) plate is given in Fig. 4(c). Here, the amplitude of the oscillation is much larger and a significant reduction in impulse is possible. For steel and aluminium the amplitude is large enough to invalidate the linear approximation used in deriving the equivalence factors (15). A non-linear analysis based on the large deflection theory of Timoschenko [4] has been carried out but is not reported here. According to the non-linear analysis, the thin plate can exhibit elastoplastic behaviour, shown by the broken line in Fig. 4(c), which takes the fluid into cavitation, not unlike the behaviour of the unsupported thin plate shown in Fig. 4(d). Multiple impacts can occur under such circumstances, as predicted earlier.

6. Elastic Support Roof Model

Bulk movement of the roof against the restraint of hold-down devices provides, along with roof flexibility, a means of relieving the pressures associated with slug impact. Whether or not significant pressure relief is realized depends on the strength of the hold-down arrangement.

We develop in this Section appropriate analytical techniques for assessing the importance of roof hold-down and examine, as an illustrative example, the clamping devices used in the COVA experiments [1], a schematic of which is given in Fig. 5(a). For a standard COVA test the roof assembly consists of a steel annular plate of thickness 15 cm, a central plug of thickness 20 cm, together with a tapered clamp ring through which pass 24 hold-down studs screwed into the base plate, itself anchored to a massive concrete raft by means of a girder framework. As the charge bubble expands, the water surface rises and upon impact with the overhead closure tends to lift the plug, roof and clamp ring assembly against the stud tensions.

A one-dimensional analogue of the COVA geometry, suitable for analysis, is illustrated in Fig. 5(b). The roof, plug and ring are represented as a lumped mass of some 1000 kg (roof flexure effects were shown in Section 5 to be of little importance). The 24 hold-down studs, which have a combined cross-sectional area close to 244 cm^2, are assumed to be fixed at their lower ends.

At impact a shock wave propogates into a liquid and tension waves are transmitted down the studs as the roof moves away under the impact loading. The conditions in the fluid behind the shock follow from the basic equations (2), (3), in the usual way:

$$P_1 = \rho_0 c \left\{\frac{U}{2} - G(z+ct)\right\} \quad ; \quad v_1 = \frac{U}{2} + G(z+ct). \tag{21}$$

In the bolts we have

$$\tilde{\sigma} = - \tilde{\rho}_0 \tilde{c}\, \tilde{G}(z+\tilde{c}t) \quad ; \quad \tilde{v} = \tilde{G}(z+\tilde{c}t) \tag{22}$$

where $\tilde{\sigma}$ is the longitudinal stress and the negative sign signifies tension. The conditions at the roof plate are obtained from (21), (22) using $z=\xi$ and $v=\tilde{v}$. The equation of motion of the plate then follows as

$$P_1 A + \tilde{\sigma}\tilde{A} = m\ddot{\xi} \tag{23}$$

in which A is the cross-sectional area of the slug and m is the roof mass. Solving, we find for the interface pressure

$$P = \rho_0 c U \left\{\frac{\tilde{\omega} + \omega e^{-(\omega+\tilde{\omega})t}}{\omega + \tilde{\omega}}\right\} \quad ; \quad \omega = \frac{\rho_0 c A}{m} \quad ; \quad \tilde{\omega} = \frac{\tilde{\rho}_0 \tilde{c}\tilde{A}}{m} \tag{24}$$

The tension waves reflect at the fixed base of each stud and identical waves return to the roof plate. These reverse as tension waves of smaller amplitude, a compression wave is transmitted down the liquid column, and the roof plate decelerates.

Soon afterwards, the initial shock wave in the liquid, reflected up from the base as a rarefaction, reaches the roof and terminates the impact. Inserting values appropriate to the "long-vessel" COVA experiments, the pressure history at the contact surface appears as in Fig. 5(c). After an initial steady decrease there is a partial recovery at the point A due to the secondary compression wave.

It transpires that the 1.4 m long hold-down studs stretch by only 1 mm during the impact event, but this is sufficient to reduce the impulse loading to the roof by 13 % compared with the fixed roof case. A similar calculation for an aluminium roof of thickness 15 cm produces an extension of 1.2 mm accompanied by an impulse reduction of 17 %.

7. Conclusions

From the evidence of the previous sections we would propose that fluid/structure interaction effects should not be ignored during the slug impact phase of an HCDA. For a roof of high flexural rigidity, bending during impact might have minimal effect on the impact pressure, but careful assessment of the strength of the hold-down arrangement is necessary as even small deflections can significantly relieve pressures in a liquid of low compressibility such as water or sodium. For roofs which are flexurally weak large differences in roof loading can occur, especially if there is plastic straining, and if momentum transfer is seriously impeded, multiple impact events are likely, governed by the collapse of large cavitated regions in the liquid.

Accordingly, a deforming roof option has been written for the containment code SEURBNUK which incorporates full coupling of roof loading and roof response during slug impact. This work, together with some applications to the modelling of roof hold-down structures is reported at this Conference by Smith, Yerkess and Adamson [5].

The assessment of the response characteristics of a reactor roof is expected to be very much more complex than that for simple homogeneous plates. A typical roof design for a pool-type reactor would involve a composite of face plates, radial and azimuthal strengthening webs, as well as concrete infill for shielding purposes. Several types of modal response would be excited during slug impact and if large deflections occur, even locally, for those structures in contact with the sodium slug, significant changes in the loading histories can be anticipated compared to those for a rigid roof. Preliminary work on the response of reactor decks to impact loads, including the effects of fluid/structure interaction, is reported at this Conference, [6], [7].

8. References

1. HOSKIN, N.E., LANCEFIELD, M.J. "The COVA Programme for the Validation of Computer Codes for Fast Reactor Containment Studies", Nucl. Eng. Des. 46, 17 (1978)
2. KENDALL, K.C., BENUZZI, A. "The COVA Programme-Validation of the Fast Reactor Containment Code SEURBNUK". Nucl. Eng. Des. 57, 79 (1980)
3. SZILARD, R. "Theory and Analysis of Plates: Classical and Numerical Methods", Prentiss Hall (1974)
4. TIMOSCHENKO, S.P., WOINOWSKY-KRIEGER, S. "The Theory of Plates and Shells", 2nd Ed., McGraw-Hill (1959)
5. SMITH, B.L., YERKESS, A., ADAMSON, J. "Status of the Coupled Fluid-Structure Dynamics Code SEURBNUK", Paper B9/1, SMiRT-7, Chicago (1983)
6. SMITH, B.L., SAURER, G., WANNER, R., "Coupled Fluid-Structure Response of a Reactor Cover to Slug Impact Loading", Paper E1/10, SMiRT-7, Chicago (1983)
7. SAURER, G., SMITH, B.L., WANNER, R. "Modelling of a LMFBR Deck Structure under Slug Impact", Paper E1/11, SMiRT-7, Chicago (1983)

Table I

A Comparison of Impulses for a Freely-Supported Roof Slab

Type	α	N	αN	Impulse (MU)	Impulse (Thin Plate)
Rigid	0.0	∞	0.0	2.0000	2.0000
15 cm Steel	0.03	10	0.3	1.5043	1.5040
15 cm Alum.	0.10	9	0.9	0.9286	0.9274
3 cm Steel	0.03	60	1.8	0.5404	0.5404
3 cm Alum.	0.10	55	5.5	0.1818	0.1818

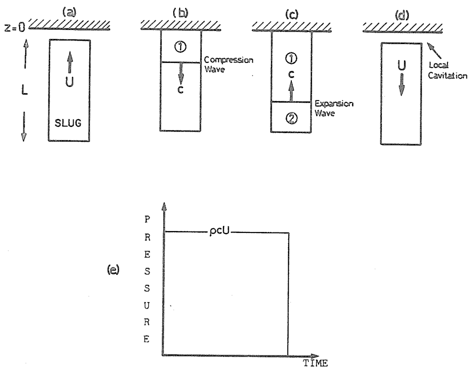

Figure 1 Impact on a Fixed, Rigid Roof

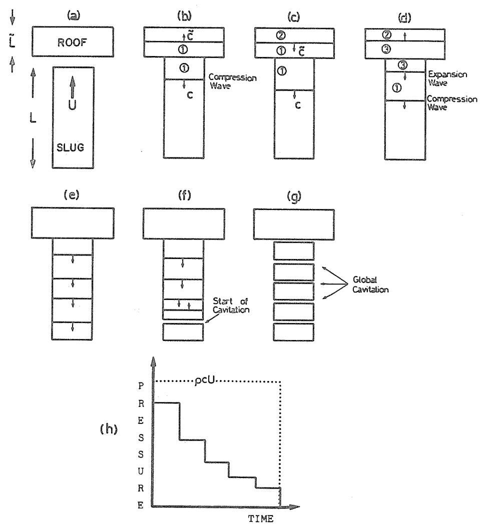

Figure 2 Impact on a Freely-Supported Roof

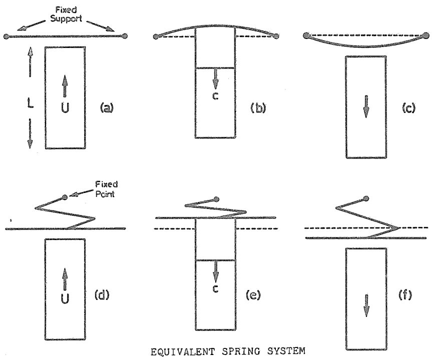

Figure 3 Impact on a Flexible Roof with Fixed Supports

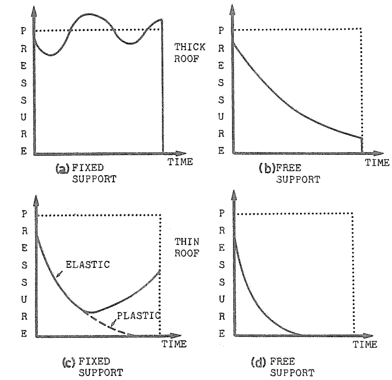

Figure 4 Pressure Histories for Fixed Support and Free Support Roof Models

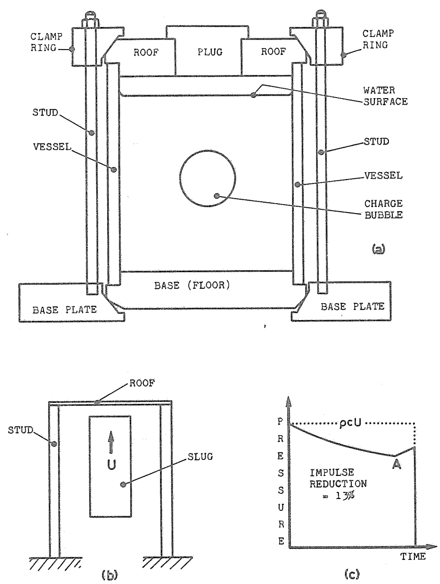

Figure 5 Analysis of Roof Hold-Down: (a) Experimental Rig
(b) Analytical Simulation
(c) Pressure Transient